Supplementary Information (SI) for Journal of Materials Chemistry C.

Defect and Carrier Engineering in Er-Doped ZnSe Enables Synergistic Electromagnetic and Charge-Transfer SERS Enhancement

Jie Li[a], Yantao Lou[a], Ze Wang[a], V Balasubramani[a], Xingchen Zhang[a], Jiaren Wu[a], Guodong Lin[a], Baofeng Zhang[b], Yuanjie Teng[a]*

[a]*National Key Laboratory of Green Chemical Synthesis and Transformation Technology, College of Chemical Engineering, Zhejiang University of Technology, Hangzhou, Zhejiang 310014, China*

[b]*Hangzhou Ecological Environment Monitoring Center, Hangzhou, Zhejiang 310013, China*

**Corresponding authors'e-mail: yuanjieteng@zjut.edu.cn*

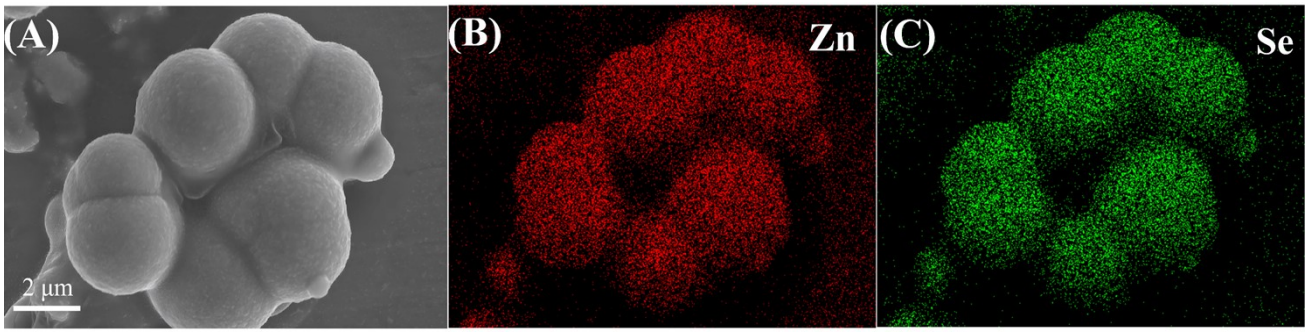

Figure S1. SEM image of ZnSe (A) and EDS mapping image (B) Zn, (C) Se

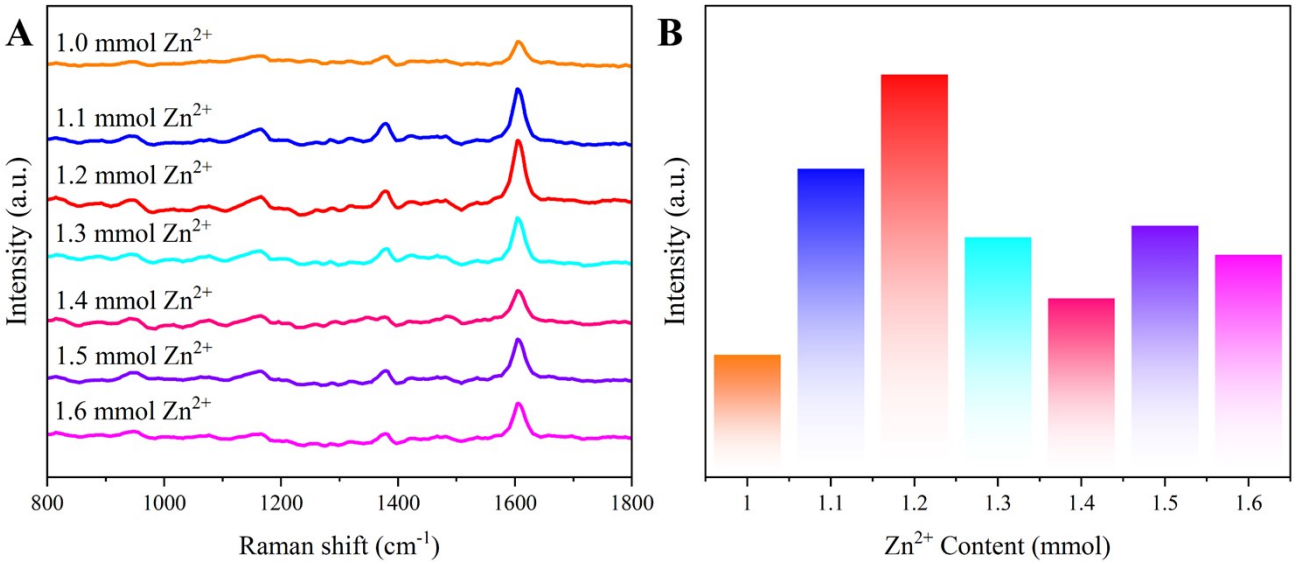

Figure S2. (A) Comparison of normalized SERS signals of MB at different Zn^{2+} contents, (B) comparison of the normalized SERS intensity of the MB Raman peak at 1600 cm^{-1}

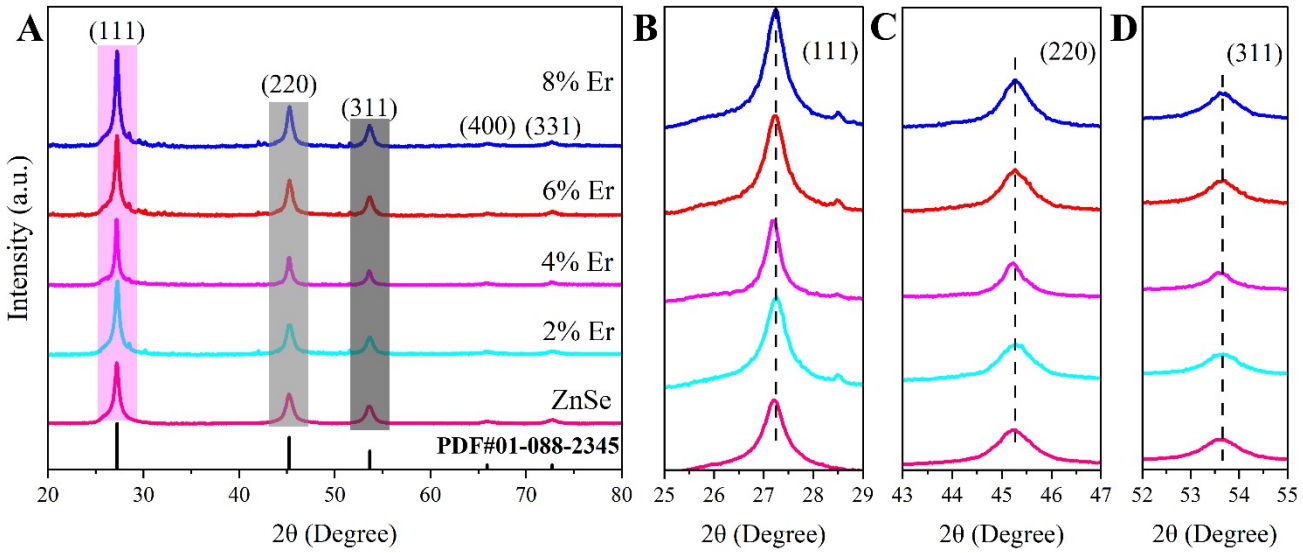

19

Figure S3. Effect of Er doping on the XRD characteristic peaks of ZnSe: (A) original diffraction patterns, (B) (111) plane, (C) (220) plane, and (D) (311) plane

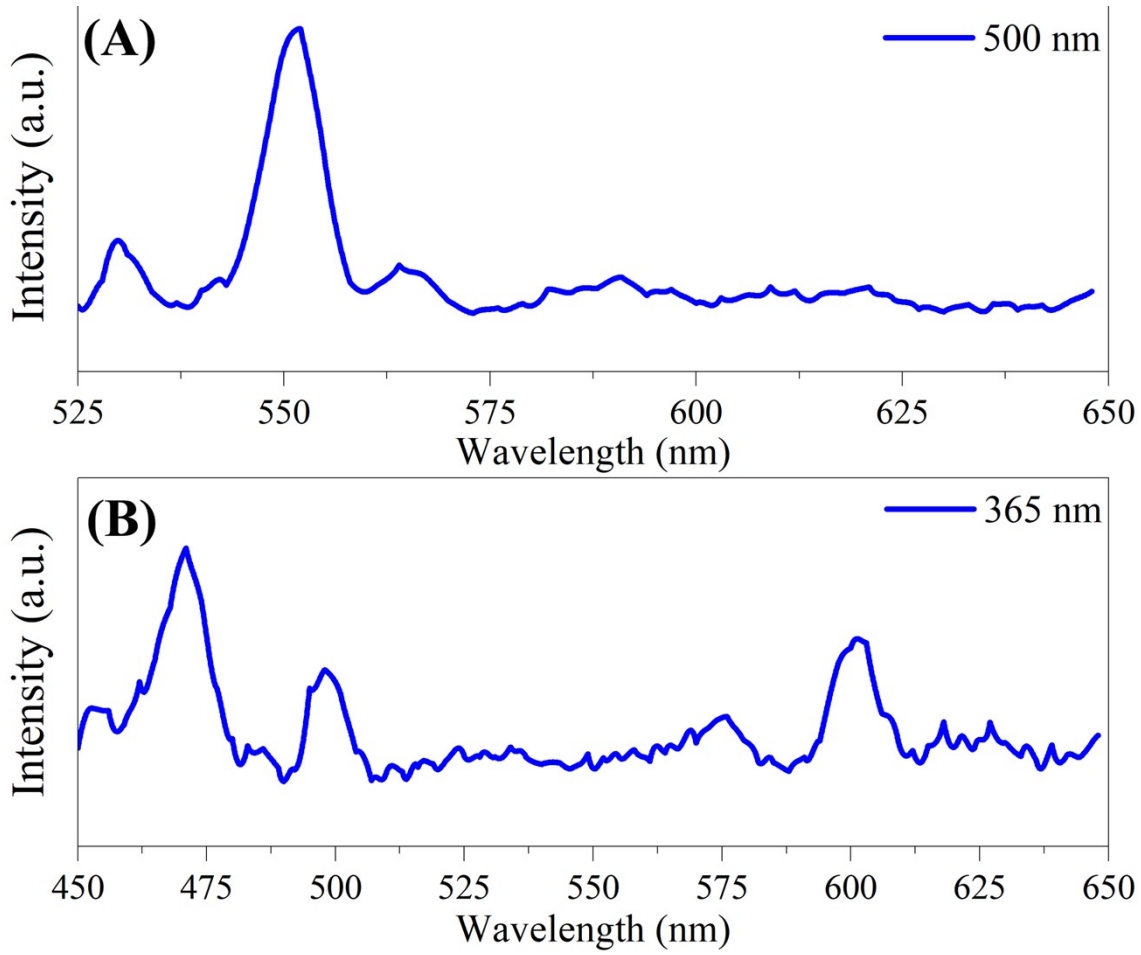

Figure S4. Fluorescence spectra of Er-ZnSe under different excitation wavelengths: (A) 500 nm, (B) 365 nm

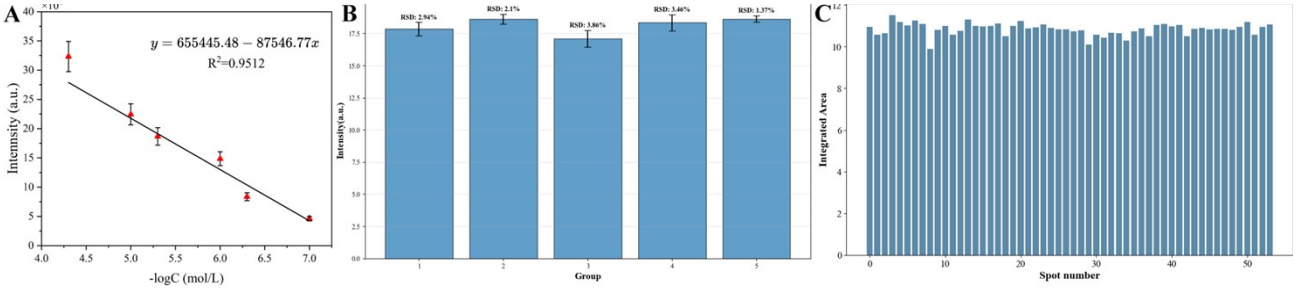

Figure S5. (A) Linear relationship between the Raman intensity of the MB characteristic peak at 1600 cm^{-1} and concentration, along with reproducibility; (B) variations among different batches; and (C) measurements at different spots

Calculation of Enhancement Factor

The enhancement factor (EF) was calculated using the data from Figure 4C and Equation S1[1]:

$$EF = \left(\frac{I_{SERS}}{I_{Raman}}\right) \times \left(\frac{c_{Raman}}{c_{SERS}}\right) \#(S1)$$

where I_{SERS} and I_{Raman} represent the Raman intensity of the probe molecule MB under SERS and normal conditions, respectively, and c_{SERS} and c_{Raman} are the corresponding concentrations of MB used in the measurements. The EF value was estimated to be approximately 1.74×10^4.

Carrier Density

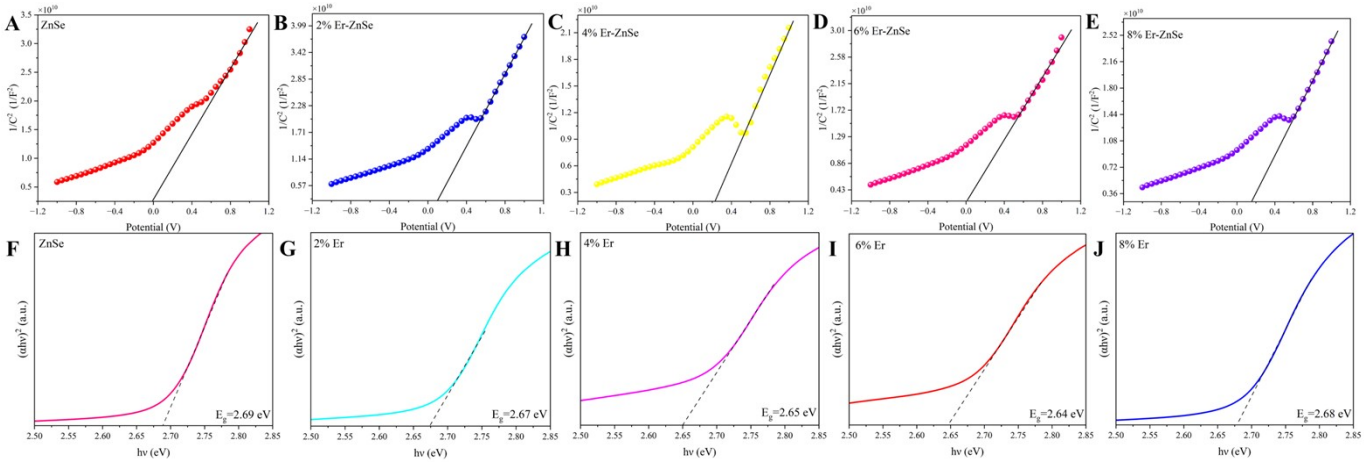

Figure S6. Mott–Schottky (M–S) plots of ZnSe with different Er doping levels: (A) ZnSe, (B) 2%, (C) 4%, (D) 6%, and (E) 8%; and UV–vis DRS: (F) ZnSe, (G) 2%, (H) 4%, (I) 6%, and (J) 8%

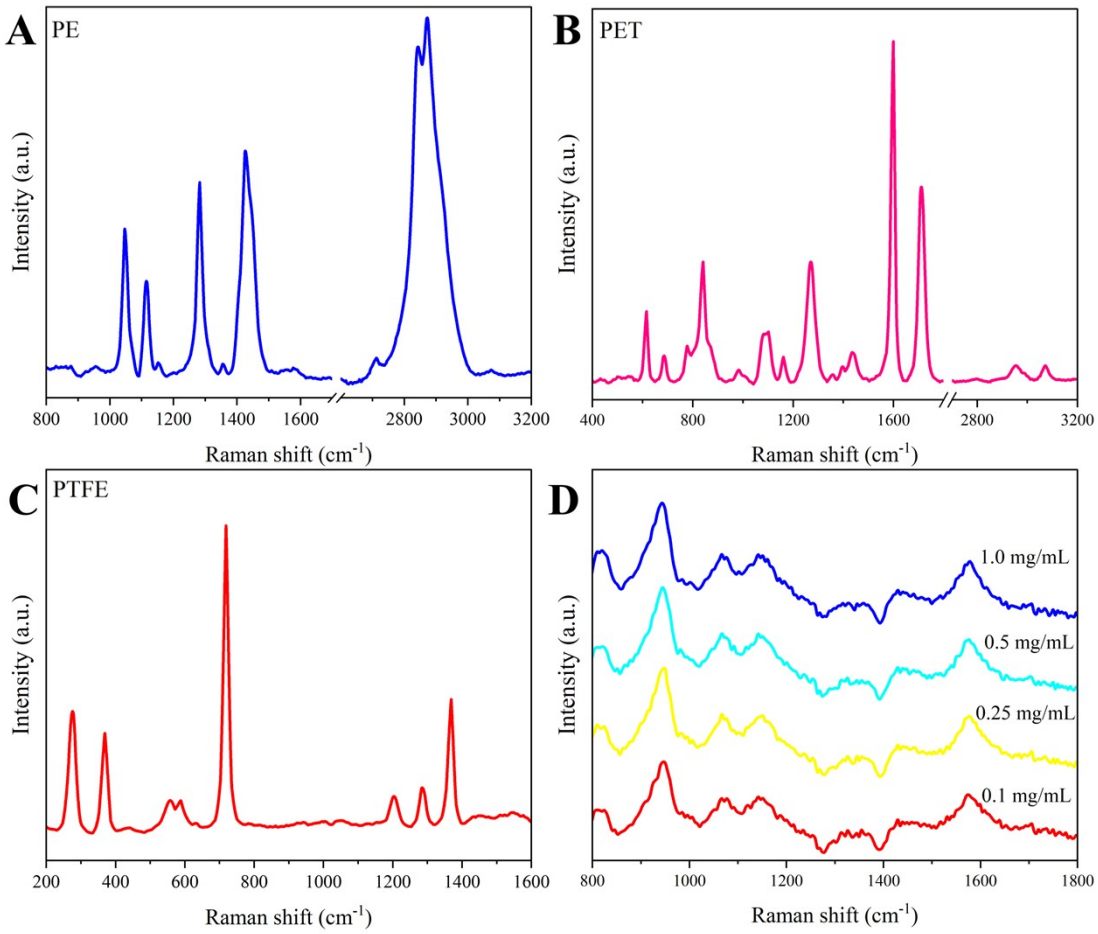

Figure S7. Raman spectra of plastics: (A) PE, (B) PET, (C) PTFE, and (D) SERS-enhanced spectrum of PTFE

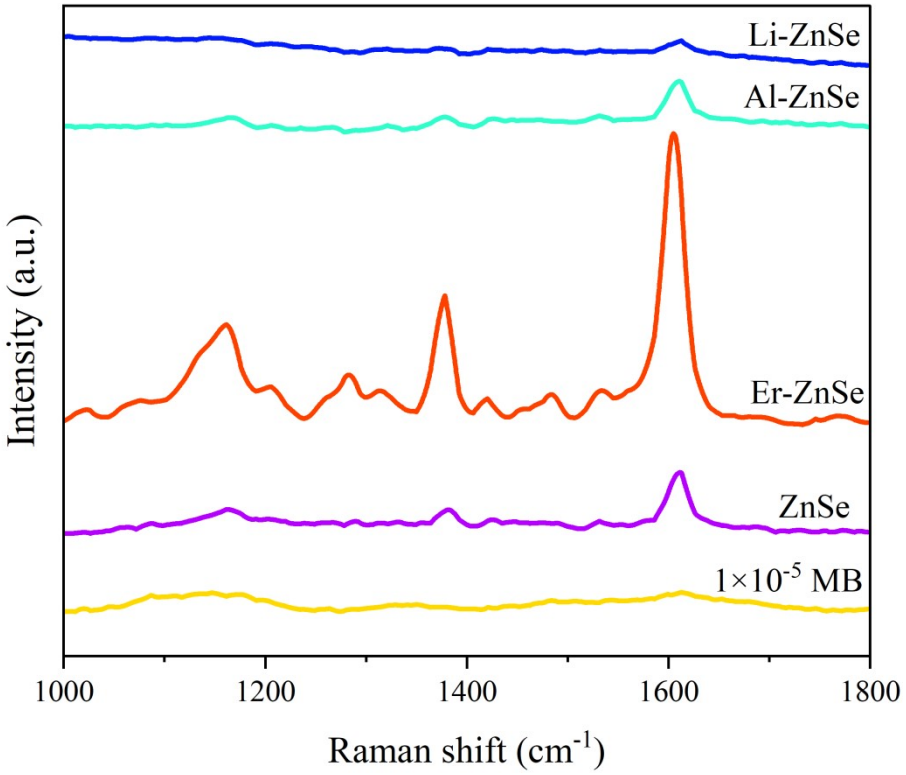

Figure S8.Comparative study of SERS performance in ZnSe with various dopants

Table S1. ρ_{CT} determined under 785 nm laser excitation

Er doped	$\rho_{CT}(1)$	$\rho_{CT}(2)$	$\rho_{CT}(3)$	$\bar{\rho_{CT}}$
0%	0.27886	0.29761	0.29048	0.28898
2%	0.27237	0.32145	0.33359	0.30913
4%	0.27053	0.25377	0.29663	0.27364
6%	0.24566	0.26039	0.26464	0.25689
8%	0.27344	0.26884	0.27047	0.27092

37 Table S2. Raman characteristic peaks of PE, PTFE, and PET and their corresponding vibrational mode assignments

Sample	Structure Simplified	Characteristic Peak (cm^{-1})	Vibration Type
PE	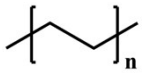	2871	CH_2 asymmetric stretching vibration
		2843	CH_2 symmetric stretching vibration
		1426	CH_2 bending vibration
		1282	CH_2 twisting vibration
		1045、1113	All-trans stretching vibration of the C–C backbone
PTFE	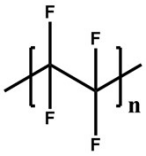	1368	Associated with the amorphous phase or defects
		1283	C–F asymmetric stretching vibration
		1203	C–F symmetric stretching vibration
		720	Symmetric stretching vibration of the C–C backbone
		557、586	CF_2 bending vibration
		369	Backbone deformation vibration of the helical chain
		277	Lattice vibration of the helical conformation
PET	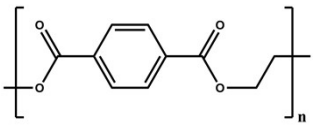	3071	Aromatic ring C–H stretching vibration
		2955	CH_2 asymmetric and symmetric stretching vibrations
		1710	C=O stretching vibration
		1600	C–C stretching vibration of the benzene ring skeleton
		1270	Coupled vibration of C(O)–O stretching and benzene ring
		840	Out-of-plane C–H bending vibration of the benzene ring
		615	In-plane deformation vibration of the benzene ring

Table S3. Comparison of the LOD and EF of this work with previous reports for SERS substrates enhancing non-resonant molecules

SERS Substrates	Probe	LOD/M	EF	Laser/nm	Mechanism
Ag-ZnSe nanowires[2]	R6G	10^{-11}	6.92×10^{7}	532	CM
Ag-ZnSe/HMM[3]	R6G	10^{-12}	3.14×10^{8}	532	CM
MoO_2/ZnSe nanocomposites[4]	MB	10^{-8}	5.03×10^{5}	532	CM
Ag@ZnSe[5]	4-MBA	--	8.79×10^{5}	514	CM+EM
Twin-ZnSe nanowires[6]	CV	10^{-8}	3.02×10^{5}	532	CM
CuPc/MoS_2[7]	MB	10^{-10}	6.29×10^{6}	532	CM
$Ti_3C_2T_x$ MXene[8]	MB	10^{-8}	6.7×10^{6}	532	CM
MoS_2/TiO_2[9]	MB	10^{-13}	2.09×10^{6}	532	CM
Er-ZnSe[This work]	MB	10^{-7}	1.74×10^{4}	785	EM+CM

References

(1) Le Ru, E. C.; Blackie, E.; Meyer, M.; *et al.* Surface Enhanced Raman Scattering Enhancement Factors: A Comprehensive Study. *J. Phys. Chem. C* **2007**, *111* (37), 13794–13803.

(2) Shafi, M.; Zhou, M.; Duan, P.; *et al.* Highly Sensitive and Recyclable Surface-Enhanced Raman Scattering (SERS) Substrates Based on Photocatalytic Activity of ZnSe Nanowires. *Sens. Actuators, B* **2022**, *356*, 131360.

(3) Shafi, M.; Duan, P.; Liu, W.; *et al.* Recyclable Surface-Enhanced Raman Spectroscopy (SERS) Platform Fabricated with Ag-Decorated ZnSe Nanowires and Metamaterial. *Sens. Actuators, B* **2023**, *380*, 133410.

(4) Liu, M.; Hu, X.; Zhang, C.; *et al.* Localized Surface Plasmon Resonance Enhanced Charge Transfer Effect in MoO_2/ZnSe Nanocomposites Enabling Efficient SERS Detection and Visible-Light Photocatalytic Degradation. *Sens. Actuators, B* **2024**, *398*, 134688.

(5) Chu, Q.; Wang, W.; Guo, S.; *et al.* Interface Design of 3D Flower-like Ag@ZnSe Composites: SERS and Photocatalytic Performance. *ACS Appl. Mater. Interfaces* **2023**, *15* (8), 11304–11313.

(6) Wang, G.; Wei, H.; Tian, Y.; *et al.* Twin-ZnSe Nanowires as Surface-Enhanced Raman Scattering Substrate with Significant Enhancement Factor upon Defect. *Opt. Express* **2020**, *28* (13), 18843–18858.

(7) Lyu, B.; Lyu, Y.; Ma, L.; *et al.* Fluorescence Quenching SERS Detection: A 2D MoS_2 Platform Modified with a Large π-Conjugated Organic Molecule for Bacterial Detection. *Laser Photonics Rev.* **2025**, *19*, 2401831.

(8) Pramanik, M.; Limaye, M. V.; Sharma, P. K.; *et al.* Improved Surface-Enhanced Raman Scattering Performance of 2D $Ti_3C_5T_x$ MXene Embedded in PVDF Film Enabled by Photoinduction and Electric Field Modulation. *ACS Appl. Mater. Interfaces* **2024**, *16* (22), 29121–29131.

(9) Quan, Y.; Su, R.; Yang, S.; *et al.* In Situ Surface-Enhanced Raman Scattering Based on MTi_{20} Nanoflowers: Monitoring and Degradation of Contaminants. *J. Hazard. Mater.* **2021**, *412*, 125209.